

# Determination of a Dimensionless Fluctuation Coefficient Using Electrochemical Impedance Spectroscopy

*M. Saitou*

Department of Mechanical Systems Engineering, University of the Ryukyus, 1 Senbaru, Nishihara-cho, Okinawa, 903-0213, Japan

E-mail: [saitou@tec.u-ryukyu.ac.jp](mailto:saitou@tec.u-ryukyu.ac.jp)

*Received:* 6 April 2019 / *Accepted:* 23 May 2019 / *Published:* 30 June 2019

---

Using the Randles circuit model, we determined that, for the impedance to fall on a straight line in a Cole–Cole plot, a dimensionless fluctuation coefficient that represents the quantity of the fluctuation in ion concentration near an electrode must be considered. The electrochemical impedance spectroscopy (EIS) measurement in a silver ferrocyanide-thiocyanate solution containing antimony potassium tartrate (APT) known as a leveling agent fell on a straight line in a Cole–Cole plot. The dimensionless fluctuation coefficient of silver ions, which was shown to be independent of the APT concentration, was determined to be 8.9 by comparison with calculations of the Randles model impedance. In addition, according to the derived formulae, exchange current density and equilibrium concentration of silver ions were determined.

---

**Keywords:** Dimensionless fluctuation coefficient, Cole–Cole plot, EIS, Randles circuit model, APT

## 1. INTRODUCTION

Electrochemical impedance spectroscopy (EIS) [1–2] provides information on electrodeposition processes interpreted in terms of equivalent electric circuits. For instance, semicircles [3–8] depicted in a Cole–Cole plot are related to the absorption and desorption of leveling additives on an electrode surface, or to multi-step charge-transfer reactions of metal ion species in a solution. However, a straight line in the Cole–Cole plot that yields a relationship between electrochemical parameters with the help of an appropriate equivalent electric circuit model has not yet been reported.

EIS becomes somewhat arbitrary [9–10] when two or more equivalent circuits sufficiently represent the experimental impedance that depends on the frequency. However, in the case of a one-step charge transfer reaction without absorbed intermediates, the equivalent circuit model is said to represent the frequency response of impedance that has been observed in practice [9].

A straight line in the Cole–Cole plot, which is interpreted as the simple one-step charge transfer

reaction under diffusion control, is represented by the Randles circuit model [11–12]. The capacitance that changes with frequency is attributed to a fluctuation in ion concentration in a solution. In this study, we demonstrate that, for the impedance to fall on a straight line in the Cole–Cole plot, a dimensionless fluctuation coefficient that represents a quantity of the fluctuation in ion concentration must be considered.

Silver electrodeposition from a solution comprising silver ferrocyanide-thiocyanate was known to obey the one-step charge transfer reaction [13]. In this study, the EIS measurements in a silver ferrocyanide-thiocyanate solution containing antimony potassium tartrate (APT) were shown to lie on a straight line in a Cole–Cole plot. Silver has attracted researchers in science and technology because of its variety of applications such as in silver nanomaterials [14–17], bacterial killing foil [18], non-noble metal catalysts [19], and the morphology of silver electrodeposits [20–23]. APT in silver electrodeposition was known as not only a leveling agent but also a pattern formation agent [24–25].

The aim of this paper is to demonstrate the following: (1) for the impedance to fall on a straight line in a Cole–Cole plot, a dimensionless fluctuation coefficient was considered; (2) the EIS measurements of a silver ferrocyanide-thiocyanate solution containing APT fell on a straight line in a Cole–Cole plot; and (3) using the derived formula, the dimensionless fluctuation coefficient, equilibrium concentration, and exchange current density of silver ions were determined.

## 2. EXPERIMENTAL SETUP

Experiments were performed using a solution that contained the following components: 25.5 g/l  $\text{AgNO}_3$ ; 72 g/l  $\text{K}_4\text{Fe}(\text{CN})_6 \cdot 3\text{H}_2\text{O}$ ; 146 g/l  $\text{KSCN}$ ; 59.3 g/l  $\text{KNaC}_4\text{H}_4\text{O}_6 \cdot 4\text{H}_2\text{O}$ ; 0, 0.75, 1.5, and 2.25 g/l  $\text{C}_8\text{H}_4\text{K}_2\text{O}_{12}\text{Sb}_2 \cdot 3\text{H}_2\text{O}$  (APT); and 31.3 g/l  $\text{K}_2\text{CO}_3$ . A solution containing  $\text{AgNO}_3$ ,  $\text{K}_2\text{CO}_3$  and  $\text{K}_4\text{Fe}(\text{CN})_6 \cdot 3\text{H}_2\text{O}$  was boiled for 30 minutes and yielded burnt umber precipitates of iron hydroxides. After the removal of the iron hydroxide, the remaining components were added into the solution. Thus, the silver ferrocyanide-thiocyanate solution containing APT was synthesized.

Polycrystalline copper square sheets with 10 mm sides were prepared for the cathode, which had a purity of 99.9 wt %. One side of the copper electrode was electrically isolated and the other side appeared to be mirror-like. A polycrystalline silver square plate with 60 mm sides, which had 99.98 wt % purity, was prepared for the anode. These electrodes were located parallel in a cell maintained at a temperature of 300 K. The silver electrode area was 72 times as large as the copper electrode area. Hence, the impedance in series of the silver electrode in the solution could be ignored in comparison with that of the copper electrode.

An LCR impedance meter connected to a personal computer through a GP-IB bus was prepared for the EIS measurements in a frequency range from 1 to 100 kHz. The LCR impedance meter imposed a sine-wave current in the cell to measure the impedance. The sine-wave current output with an amplitude of  $0.1\text{mA}/\text{cm}^2$  was chosen to give rise to a cell voltage less than 5 mV. Hence, the cathode potential was lower than 5 mV.

### 3. RESULTS AND DISCUSSION

#### 3.1 Dimensionless fluctuation coefficient derived from the Randles circuit model

We first made an analytical attempt to derive a condition that ensures that the impedance falls on a straight line in a Cole–Cole plot using the Randle circuit model [11] that includes the Warburg impedance.

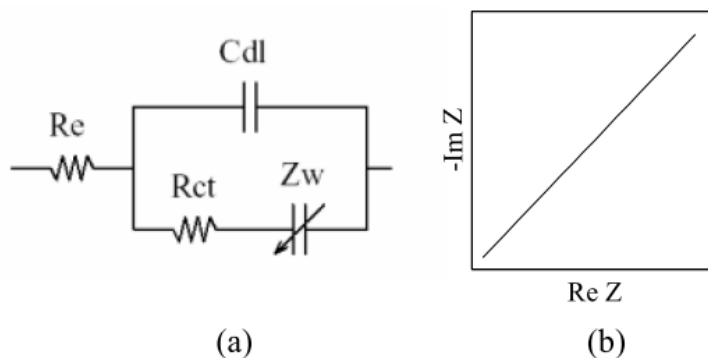


**Figure 1.** Equivalent electric circuit model: (a) Randles circuit model and (b) Straight line in the Cole–Cole plot.

The Randles circuit model comprising the solution resistance  $R_e$ , electric double layer capacitance  $C_{dl}$ , resistance due to the charge transfer reaction  $R_{ct}$ , and Warburg impedance  $Z_w$  is shown in Fig.1 (a). For a sine wave input with an angular frequency  $\omega$ , the impedance  $Z$  in the Randles circuit model can be written as

$$Z = R_e + \frac{1}{j\omega C_{dl} + \frac{1}{R_{ct} + Z_w}}, \tag{1}$$

where  $j$  is the purely imaginary number. The Warburg impedance [12] is represented by

$$Z_w = \frac{(1-j)\sigma}{\sqrt{\omega}}, \tag{2}$$

and the Warburg coefficient is given by

$$\sigma = \frac{RT}{z^2 F^2 c_o \sqrt{2D}}, \tag{3}$$

where  $z$  is the valence number,  $F$  is Faraday’s constant,  $R$  is the gas constant,  $D$  is the diffusion constant,  $T$  is the absolute temperature, and  $c_o$  is the equilibrium concentration of ions in the solution. For  $\zeta \ll RT/zF$  where  $\zeta$  is the cathode potential, the resistance for the charge transfer reaction,  $R_{ct}$  becomes

$$R_{ct} = \frac{RT}{i_0 z F}, \quad (4)$$

where  $i_0$  is the exchange current density.

Next, we derived the formula required for the impedance to lie on a straight line in the Cole–Cole plot as shown in Fig. 1 (b) even if some additives are added to the solution. Equation (1) has the following form:

$$Z = R_e + \frac{b}{a} - j \frac{c}{a}, \quad (5)$$

where  $a$ ,  $b$ , and  $c$  are real numbers. We define a change in the impedance and its components, caused by the concentration change in the ions in the solution, as  $\Delta Z$ ,  $\Delta b$ , and  $\Delta c$ . The following equation should be satisfied for the impedance to fall on the single straight line passing through the origin in the Cole–Cole plot,

$$\frac{\text{img } Z}{\text{real } Z} = \frac{\text{img } (Z + \Delta Z)}{\text{real } (Z + \Delta Z)}. \quad (6)$$

This equation only means that the slope in the Cole–Cole plot is not changed even if the change in the impedance occurs. Substituting Eq. (5) into Eq. (6), we have

$$\frac{\Delta b}{b} = \frac{\Delta c}{c}, \quad (7)$$

where  $b = R_{ct} + \frac{\sigma}{\sqrt{\omega}}$  and  $c = \frac{\sigma}{\sqrt{\omega}} + 2C_{dl}\sigma^2 + \omega C_{dl}R_{ct}^2 + 2\sqrt{\omega}C_{dl}R_{ct}\sigma$ . Equation (7) leads

$$\frac{\Delta R_{ct} + \frac{\Delta\sigma}{\sqrt{\omega}}}{R_{ct} + \frac{\sigma}{\sqrt{\omega}}} = \frac{\frac{\Delta\sigma}{\sqrt{\omega}} + 2(\sigma^2 \Delta C_{dl} + 2C_{dl}\sigma\Delta\sigma) + \omega A_1 + 2\sqrt{\omega}A_2}{\frac{\sigma}{\sqrt{\omega}} + 2C_{dl}\sigma^2 + \omega C_{dl}R_{ct}^2 + 2\sqrt{\omega}C_{dl}R_{ct}\sigma}, \quad (8)$$

where  $A_1 = \Delta C_{dl}R_{ct}^2 + 2C_{dl}R_{ct}\Delta R_{ct}$  and  $A_2 = C_{dl}R_{ct}\Delta\sigma + C_{dl}\Delta R_{ct}\sigma + \Delta C_{dl}R_{ct}\sigma$ . Here, the solution resistance  $R_e$  does not vary with the additive concentration, and the terms with higher orders than the second order terms can be negligible. If Equation (8) always hold true irrespective of  $\omega$ , Equation (8) should satisfy

$$\begin{aligned} \sigma\Delta C_{dl} + C_{dl}\Delta\sigma &= 0, \\ \Delta C_{dl}R_{ct} + C_{dl}\Delta R_{ct} &= 0. \end{aligned} \quad (9)$$

Equation (9) yields

$$\sigma / R_{ct} = \text{const.} \quad (10)$$

Substituting Eqs. (3) and (4) into Eq. (10), we define the dimensionless fluctuation coefficient of an ion concentration as

$$C_f = \frac{i_o}{\sqrt{2D}c_o} \frac{zF}{zF}. \quad (11)$$

The Warburg impedance dependent on the frequency  $\omega$  is attributed to a fluctuation in the ion concentration. The numerator in Eq. (11) represents the fluctuation in the ions caused by the mole number of ions that can crystallize on the electrode during 1 s. The denominator in Eq. (11) represents the fluctuation in the ions caused by the mole number of ions that can diffuse during 1 s.

If the fluctuation in ion concentration near the cathode is attributed to crystallized ions, the coefficient  $C_f$  defines how large the fluctuation in the ion concentration is. When  $C_f$  approaches zero, the fluctuation reaches zero because the high concentration of ions quickly responds to a decrease in the number of ions in the solution due to the crystallized ions. Hence, the impedance  $Z$  in Eq. (1) depicts a semi-circle on a Cole–Cole plot. On the other hand, for  $C_f \gg 1$ , the impedance  $Z$  depicts a straight line perpendicular to the  $\text{Re } Z$  axis when the frequency  $\omega$  approaches zero, and it reaches  $R_e$  when the frequency  $\omega$  approaches zero according to Eqs. (1) and (3). When  $C_f$  has an intermediate value, the fluctuation in the ion concentration occurs owing to the Warburg impedance, and a straight line will be depicted on a Cole–Cole plot.

The fluctuation in ion concentrations near the cathode causes a change in the number of atoms arriving at the surface of the anode and causes the fluctuation in the surface height of the electrodeposit, i.e., an unstable surface.

Within the framework of film growth, governing equations including a fluctuation in the deposition process,  $\eta(x, t)$  have been studied [26]. For example, the KPZ equation in one dimension [27] has the following form,

$$\frac{\partial h}{\partial t} = \nu \nabla^2 h + \frac{\lambda}{2} (\nabla h)^2 + \eta, \quad (12)$$

$$\langle \eta(x, t) \eta(x', t') \rangle = 2D \delta(x - x') \delta(t - t'), \quad (13)$$

where  $h$  is the height of a deposited layer,  $\nu$  is the surface tension, and  $\lambda$  is the constant. Equation (13) implies no correlation of  $\eta(x, t)$  in space  $x$  and time  $t$ . The term  $\eta(x, t)$  is interpreted as a noise related to diffusion combined with the diffusion coefficient,  $D$  and affects the film growth and the surface roughness of the deposit [28]. Equation (11) also indicates the presence of a fluctuation in the ion concentration that affects the film height. However, a relationship between the term  $\eta(x, t)$  and the fluctuation in the ion concentration has not been theoretically derived.

3.2 EIS measurement in the silver ferrocyanide-thiocyanate solution containing APT

Figure 2 shows the Cole–Cole plot in a frequency range from 1 to 100 kHz for the four different concentrations of APT in the silver ferrocyanide-thiocyanate solution. A change in the quantity of the impedance dependent on the APT concentration can be observed, but all the data almost fall on the simple straight line. A partially resolved semicircle [29] at high angular frequencies, which is due to the presence of an electric double layer, very weakly emerges in the Cole–Cole plot. This suggests that the Fermi level of the electron in the cathode is not so different from the chemical potential of the solution. The real and imaginary parts of the impedance at low angular frequencies lie on the straight line whose slope is not 45° owing to the presence of the capacitance, which depends on the frequency. The requirement for Eq. (10) is that all the data fall on the straight line irrespective of the additive concentration. Figure 2 shows that the requirement is satisfied.

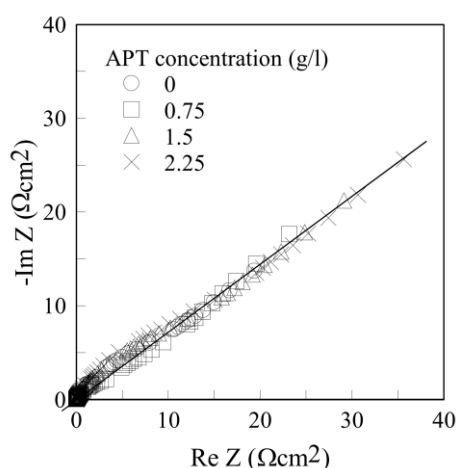


**Figure 2.** Cole–Cole plots within a frequency range from 1 to 100 kHz for the four APT concentrations. The straight line was drawn to guide the eyes.

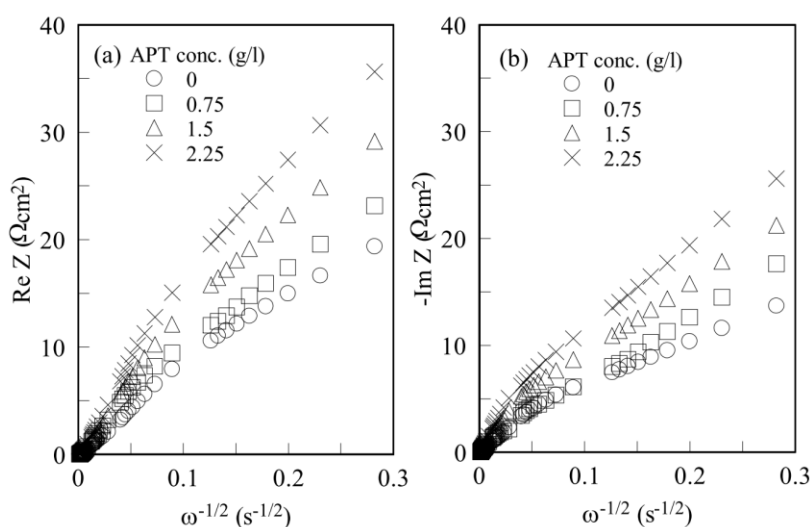


**Figure 3.** Typical plots of the real and imaginary parts of the impedance dependent on  $\omega^{-1/2}$ : (a) Real part of the impedance vs.  $\omega^{-1/2}$  and (b) Imaginary part of the impedance vs.  $\omega^{-1/2}$ .

In Fig. 3, the real and imaginary parts of the impedance were plotted as a function of the angular frequency  $\omega^{-1/2}$  so that a detailed interpretation of the impedance behavior could be made. The two parts increase with the concentration of APT and those at the low angular frequencies are linearly proportional to  $\omega^{-1/2}$ . This shows that the experimental results were consistent with the Warburg impedance.

The approximation condition  $\zeta \ll RT/zF$  was valid for this study owing to  $\zeta < 5\text{mV} < RT/zF = 25.8\text{mV}$  at a temperature of 300 K where 5 mV was the maximum cell voltage when the sine-wave current with an amplitude value of  $0.1\text{mA/cm}^2$  was applied over the cell as explained in the Experimental setup. The Randles circuit model includes the Warburg impedance, which means that chemical ion species in the solution are transported by diffusion. No semicircle appears in the Cole–Cole plot at high angular frequencies and cathode potentials. The condition  $\zeta \ll 5\text{mV}$  means that the Fermi level of the electron in the electrode was almost equal to the chemical potential of the solution near the electric double layer. Hence, the applied potential at the cathode was very small; however, the electrochemical reaction from silver ions to silver atoms occurred. That is, we could observe the resistance due to the charge transfer reaction of silver ions.

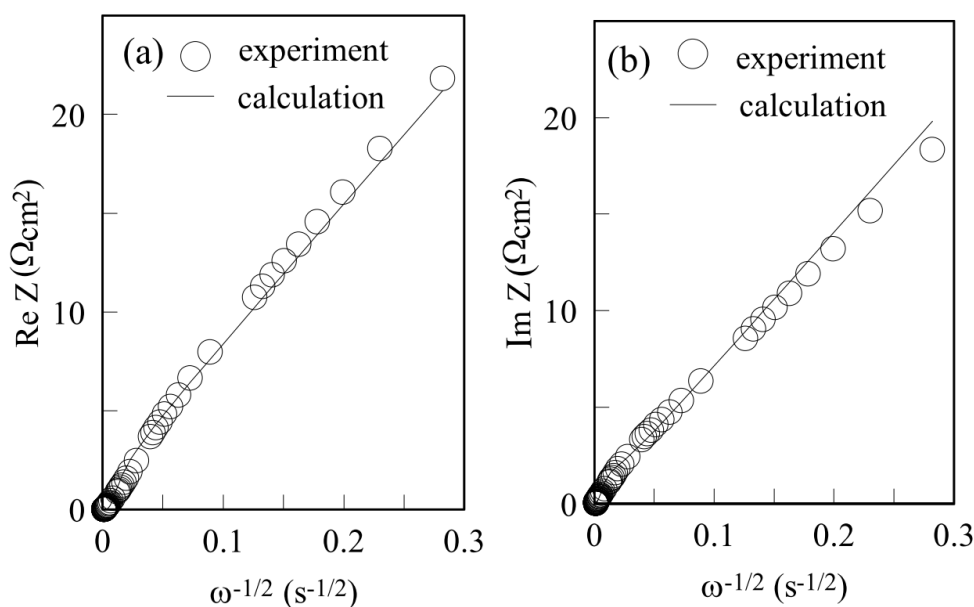


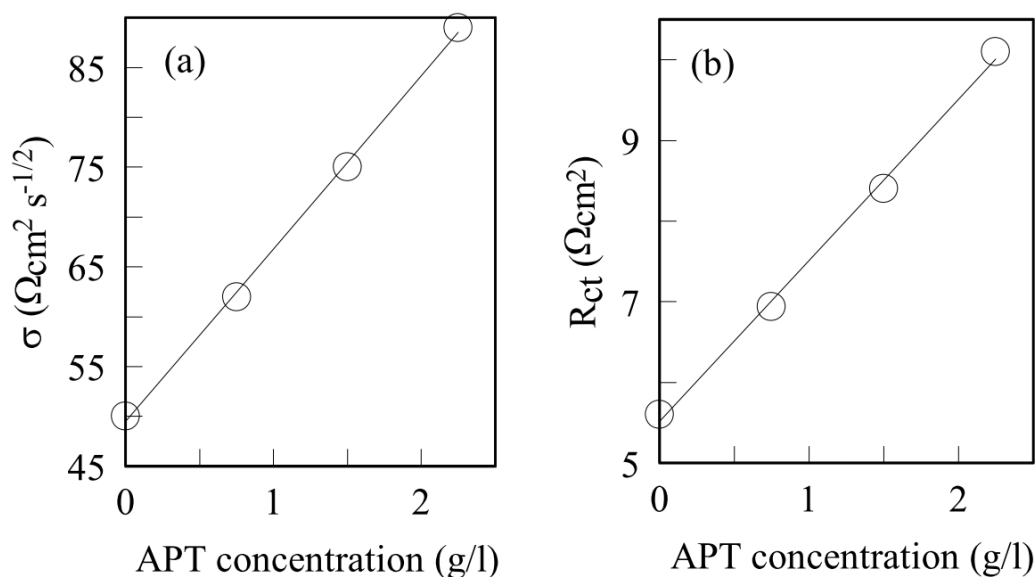
**Figure 4.** Typical experimental and calculated impedances dependent on  $\omega^{-1/2}$ . The solid lines and open circles indicate the calculated and the experimental values for the silver ferrocyanide-thiocyanate electrolyte containing 1.5g/l APT, respectively. The parameters used in the calculation were  $R_e = 0\ \Omega$ ,  $\sigma = 75\ \Omega\text{cm}^2\text{s}^{-1/2}$ ,  $R_{ct} = 8.4\ \Omega\text{cm}^2$ , and  $C_{dl} = 10^{-4}\ \text{F}$ . (a) Real part of impedance vs.  $\omega^{-1/2}$ ; (b) Imaginary part of impedance vs.  $\omega^{-1/2}$

The typical calculation results based on Eqs. (1)-(4) were shown in Fig. 4. The impedance measured in the silver ferrocyanide-thiocyanate solution containing 1.5g/l APT was also plotted in Fig.4. The real and imaginary parts in the calculation were in good agreements with those in the experiment. As the Warburg impedance represents the electrical behavior of ion transport by diffusion, no chemical reaction is considered to occur in the diffusion layer owing to the presence of APT [30]. In addition,

Figure 2 also shows that some complicated reactions by multi-step reactions and absorbed intermediates did not occur. Hence, the kinetic reactions in the silver solution containing APT can be described by the simple charge transfer reaction under diffusion control [13]. The equivalent circuit approach in this experiment has a good relation to what occurs in practice.

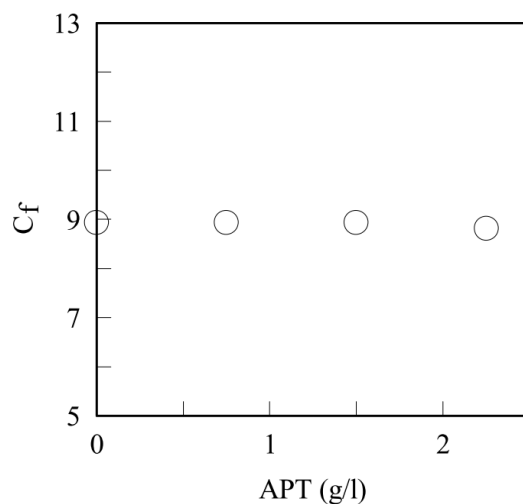
### 3.3 Determination of the dimensionless fluctuation parameter $C_f$

Figure 5 shows the calculated values of  $\sigma$  and  $R_{ct}$  best fitted to the experimental impedance as shown in Fig. 4 for the different concentrations of APT. The two parameters linearly increase with APT concentration. Hence, the results of  $\sigma$  and  $R_{ct}$  support Eq. (10).



**Figure 5.** Dependence of  $\sigma$  and  $R_{ct}$  on the APT content. These values were best fitted to the experimental impedances in Fig.3. The straight line was a guide for the eyes. (a)  $\sigma$  vs. APT concentration, (b)  $R_{ct}$  vs. APT concentration.

Figure 6 shows the dimensionless fluctuation coefficients  $C_f$  that had a constant value of 8.9 independent of the APT concentration. If there is no fluctuation in silver ions, the value of  $C_f$  becomes zero. The concentration fluctuation in silver ions occurred and was observed as the capacitance that depends on the frequency. In electrodeposition, the concentration fluctuation of the silver ions near the substrate causes the rough surface of silver electrodeposits.



**Figure 6.** Dependence of  $C_f$  on the APT concentration.

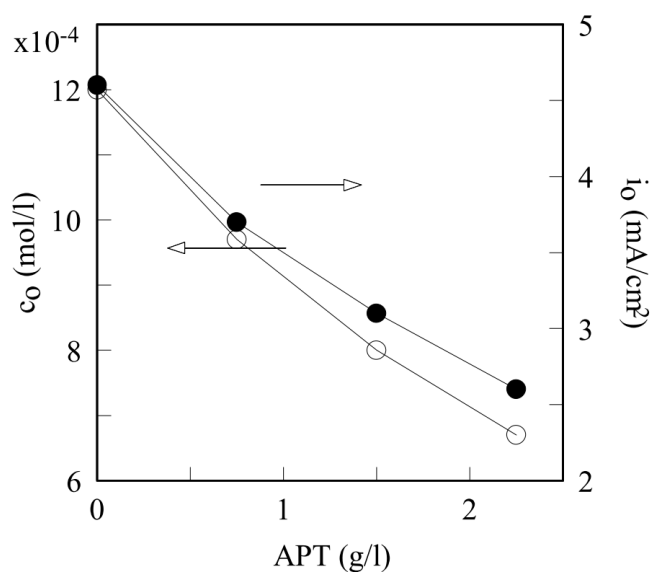


**Figure 7.** Plot of the exchange current density,  $i_o$  and thermal equilibrium concentration of silver ions,  $c_o$  for the four different APT concentration.

According to Eqs. (3) and (4), the equilibrium concentration of silver ions,  $c_o$ , and the exchange current density,  $i_o$  were obtained as shown in Fig. 7. Here, the diffusion coefficient  $D$  was assumed to be  $10^{-5}$  s/cm<sup>2</sup> [31]. The equilibrium concentration of silver ions and the exchange current density decrease with APT concentration. These results suggest that the activity of silver ions in the solution and the crystallization of silver ions tended to be suppressed by the presence of APT. As the Cole–Cole plot in Fig. 2 comprises only the straight line and no semi-circle, the desorption and absorption of APT may not occur at the cathode. Hence, the effect of APT on silver deposition is different from that of other leveling agents such as coumarin [10] that inhibit growth by adsorption and desorption at cathode electrodes.

#### 4. CONCLUSIONS

For the impedance to fall on a straight line in the Cole–Cole plot, a dimensionless fluctuation coefficient that represents the quantity of concentration fluctuation in a solution near an electrode must be considered. The EIS measurements in the silver ferrocyanide-thiocyanate electrolyte containing APT fell on a straight line in the Cole–Cole plot. According to the derived formulae, the dimensionless fluctuation coefficient, exchange current density, and equilibrium concentration of silver ions were determined.

#### References

1. B. E. Conway and R. E. White, *Modern Aspects of Electrochemistry*, Kluwer/Plenum, New York, 2002.
2. F. Lu, B. Song, P. He, Z. Wang, and J. Wang, *RSC Adv.*, 7 (2017) 13742.
3. R. D. Armstrong and M. Henderson, *J. Electroanal. Chem.*, 39 (1972) 81.
4. J. Bressan and R. Wiart, *J. Appl. Electrochem.*, 9 (1979) 615.
5. R. Wiart, *Electrochim. Acta*, 10 (1990) 1587.
6. B. C. Baker and A. C. West, *J. Electrochem. Soc.*, 144 (1997) 164.
7. Q. Cheng and Z. Chen, *Int. J. Electrochem. Soc.*, 8 (2013) 8282.
8. J. Jalili and V. Tricoli, *Front. Energy Res.*, 2 (2014) 1.
9. J. O'M Bockris, A. K. N. Reddy, and M. G-Aldeco, *Modern Electrochemistry*, Vol. 2 A, Kluwer Academic, New York, 2000.
10. B. E. Conway, *Electrochemical Supercapacitors*, Kluwer Academic, New York, 1999.
11. J. E. Randles, *Discuss. Faraday Soc.*, 1 (1947) 11.
12. P. K. Pandey, S. N. Sahu, and S. Chandra, *Handbook of Semiconductor Electrodeposition*, Marcel Dekker Inc., New York, 1996.
13. I. Krastev, A. Zielonka, S. Nakabayashi, and K. Inokuma, *J. Appl. Electrochem.*, 312 (2001) 1047.
14. D. Zhang, Y. Tang, F. Jiang, Z. Han, and J. Chen, *Appl. Sur. Sci.*, 369 (2016) 178.
15. A. Kobler, T. Beuth, T. Klöffel, R. Prang, M. Moosmann, T. Scherer, S. Walheim, H. Hahn, C. Kübel, B. Meyer, T. Schimmel, and E. Bitzek, *Acta. Mater.*, 92 (2015) 299.
16. I. Pedre, F. Battaglini, G. J. L. Delgado, M. G. S-Loredo, and G. A. González, *Sensor Actuat. B*, 211 (2015) 515.
17. M. Zhang, Y. Zhang, P. Liu, M. Chen, Z. Cai, and F. Cheng, *Int. J. Electrochem. Sci.*, 10 (2015) 4314.
18. M. Hoop, Yu. Shen, Z. Chen, F. Mushtaq, L. M. Luliano, M. S. Sakar, A. Petruska, M. J. Loessner, B. J. Nelson, and S. Pane, *Adv. Funct. Mater.*, 26 (2016) 1063.
19. K. Lee, M. S. Ahmed, and S. Jeon, *J. Power Sources*, 288 (2015) 261.
20. R. Sivasubramanian and M. V. Sangaranarayanan, *Sensor Actuat. B*, 213 (2015) 92.
21. M. Chirea, S. S. E. Collins, X. Wei, and P. Mulvaney, *J. Phys. Chem. Lett.*, 5 (2014) 4331.
22. B. Liu and M. Wang, *Int. J. Electrochem. Sci.*, 8 (2013) 8572.
23. K. I. Popov, P. M. Živković, and N. D. Nikolić, *Int. J. Electrochem. Sci.*, 7 (2012) 686.
24. S. Striveeraghaven, R. M. Krishnan, and S. R. Natarajan, *Metal Finishing*, 87 (1989) 115.
25. V. Skučas, I. Valentėlis, J. Gilaitytė, A. Kindury, and G. Krivaitė, *Mater. Sci.*, 9 (2003) 178.
26. A. -L. Barabási and H. E. Stanley, *Fractal Concepts in Surface Growth*, Cambridge Uni. Pr. (1995).
27. M. Kardar, G. Parisi and Y. -C. Zhang, *Phys. Rev. Lett.*, 56 (1986) 889.
28. M. Saitou, *Phys. Rev. B*, 66 (2002) 073416.
29. F. Rashwan, *Am. J. Appl. Sci.*, 2 (2005) 1595.

30. M. Saitou and Y. Fuoka, *Electrochim. Acta*, 50 (2005) 5044.
31. R. R. Johnston and M. Spiro, *J. Phys. Chem.*, 71 (1967) 3784.

© 2019 The Authors. Published by ESG ([www.electrochemsci.org](http://www.electrochemsci.org)). This article is an open access article distributed under the terms and conditions of the Creative Commons Attribution license (<http://creativecommons.org/licenses/by/4.0/>).